AD-A172 176 MAGNETOHYDRODYNAMIC MODELLING OF SOLAR DISTURBANCES IN THE INTERPLANETARY MEDIUM(U) NATIONAL OCEANIC AND ATMOSPHERIC ADMINISTRATION BOULDER CO SP.. M DRYER

1/1

UNCLASSIFIED DEC 85 AFGL-TR-86-0161 F/G 3/2 NL

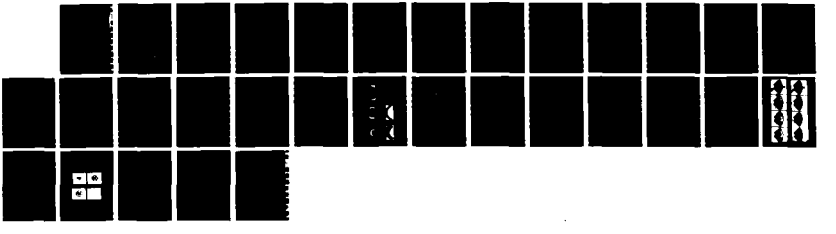

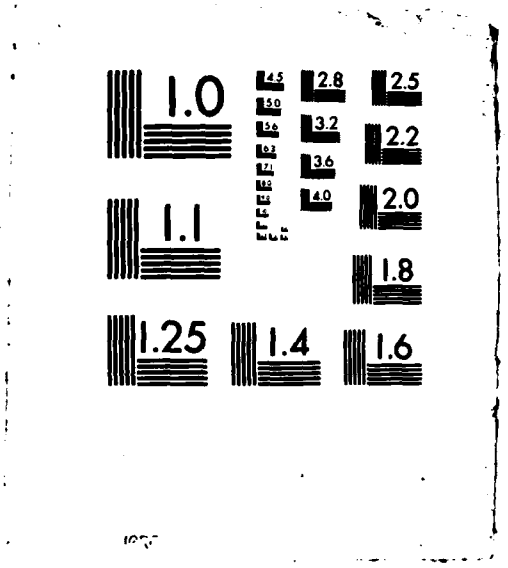
1.0
1.1
1.25
1.4
1.6
1.8
2.0
2.2
2.5
2.8
3.2
3.6
4.0
4.5
5.0

(12)

AFGL-TR-86-0161

Magnetohydrodynamic Modelling of Solar Disturbances in the Interplanetary Medium

M. Dryer

NOAA/ERL
Space Environment Laboratory
325 Broadway
Boulder, Colorado 80303

December 1985

Final Report
April 1983 - December 1985

APPROVED FOR PUBLIC RELEASE; DISTRIBUTION UNLIMITED

AIR FORCE GEOPHYSICS LABORATORY
AIR FORCE SYSTEMS COMMAND
UNITED STATES AIR FORCE
HANSCOM AIR FORCE BASE, MASSACHUSETTS 01731

"This technical report has been reviewed and is approved for publication"

Don F. Smart
Contract Manager

E. G. Mullen
Chief, Space Particles Environment Branch

FOR THE COMMANDER

Rita C. Saglyn
Director, Space Physics Division

This report has been reviewed by the ESD Public Affairs Office (PA) and is releasable to the National Technical Information Service (NTIS).

Qualified requestors may obtain additional copies from the Defense Technical Information Center. All others should apply to the National Technical Information Service.

If your address has changed, or if you wish to be removed from the mailing list, or if the addressee is no longer employed by your organization, please notify AFGL/DAA, Hanscom AFB, MA 01731. This will assist us in maintaining a current mailing list.

Unclassified

SECURITY CLASSIFICATION OF THIS PAGE

REPORT DOCUMENTATION PAGE AD-A172176

1a. REPORT SECURITY CLASSIFICATION: Unclassified	1b. RESTRICTIVE MARKINGS
2a. SECURITY CLASSIFICATION AUTHORITY	3. DISTRIBUTION/AVAILABILITY OF REPORT: Available for public release Distribution unlimited
2b. DECLASSIFICATION/DOWNGRADING SCHEDULE	
4. PERFORMING ORGANIZATION REPORT NUMBER(S)	5. MONITORING ORGANIZATION REPORT NUMBER(S): AFGL-TR-86-0161
6a. NAME OF PERFORMING ORGANIZATION: Space Environment Laboratory NOAA/ERL; 6b. OFFICE SYMBOL (If applicable)	7a. NAME OF MONITORING ORGANIZATION: Air Force Geophysics Laboratory
6c. ADDRESS (City, State and ZIP Code): 325 Broadway Boulder Colorado 80303	7b. ADDRESS (City, State and ZIP Code): Hanscom Air Force Base Bedford, MA 01731
8a. NAME OF FUNDING/SPONSORING ORGANIZATION; 8b. OFFICE SYMBOL (If applicable): PHP	9. PROCUREMENT INSTRUMENT IDENTIFICATION NUMBER: Project orders ESD-3-935, ESD-4-619 ESD-5-618
8c. ADDRESS (City, State and ZIP Code)	10 SOURCE OF FUNDING NOS: PROGRAM ELEMENT NO. 61102F; PROJECT NO 2311; TASK NO. G1; WORK UNIT NO DD
11 TITLE (Include Security Classification): Magnetohydrodynamic Modelling of Solar Disturbances (Con't)	
12. PERSONAL AUTHOR(S): M. Dryer	
13a. TYPE OF REPORT: Final; 13b. TIME COVERED: FROM Apr 83 TO Dec 85; 14 DATE OF REPORT (Yr., Mo., Day): 85 December; 15 PAGE COUNT: 28	
16. SUPPLEMENTARY NOTATION	

17 COSATI CODES		
FIELD	GROUP	SUB GR
03	01	
03	02	

18 SUBJECT TERMS (Continue on reverse if necessary and identify by block number): MHD modeling, Solar flare generated Shock, Solar-Terrestrial Physics, interplanetary medium

19 ABSTRACT

We have scientifically constructed a series of interplanetary MHD models that comprise the foundations for a composite solar-terrestrial environment model. These models, unique in the field of solar wind physics, include both 2-1/2D as well as 3D time-dependent codes that will lead to future operational status. We have also developed a geomagnetic storm forecasting strategy, referred to as the Solar-Terrestrial Environment Model (STEM/2000), whereby these models would be appended in modular fashion to solar, magnetosphere, ionosphere, thermosphere, and neutral atmosphere models. We stress that these models, while still not appropriate at this date for operational use, outline a strategy or blueprint for the future. This strategy, if implemented in its essential features, offers a high probability for technology transfer from theory to operational testing within, approximately, a decade. It would ensure that real-time observations would be used to drive physically-based models that outputs of which would be used by space environment forecasters.

20 DISTRIBUTION AVAILABILITY OF ABSTRACT: UNCLASSIFIED/UNLIMITED X SAME AS RPT. ☐ DTIC USERS ☐	21 ABSTRACT SECURITY CLASSIFICATION: Unclassified
22a NAME OF RESPONSIBLE INDIVIDUAL: Don F. Smart	22b TELEPHONE NUMBER (Include Area Code): 617-377-3978; 22c OFFICE SYMBOL: PHP

DD FORM 1473, 83 APR EDITION OF 1 JAN 73 IS OBSOLETE.

Unclassified

SECURITY CLASSIFICATION OF THIS PAGE

Cont of Block 11:

in the Interplanetary Medium

Accession For	
NTIS GRA&I	☒
DTIC TAB	☐
Unannounced	☐
Justification	
By	
Distribution/	
Availability Codes	
Dist	Avail and/or Special
A-1	

ABSTRACT

We have scientifically constructed a series of interplanetary MHD models that comprise the foundations for a composite solar-terrestrial environment model. These models, unique in the field of solar wind physics, include both 2-1/2D as well as 3D time-dependent codes that will lead to future operational status. We have also developed a geomagnetic storm forecasting strategy, referred to as the Solar-Terrestrial Environment Model (STEM/2000), whereby these models would be appended in modular fashion to solar, magnetosphere, ionosphere, thermosphere, and neutral atmosphere models. We stress that these models, while still not appropriate at this date for operational use, outline a strategy or blueprint for the future. This strategy, if implemented in its essential features, offers a high probability for technology transfer from theory to operational testing within, approximately, a decade. It would ensure that real-time observations would be used to drive physically-based models that outputs of which would be used by space environment forecasters.

A Bibliography of papers is appended, with listing by first author for easy reference. A Summary comprises the balance of this Final Report in which the various papers are categorized with a description of their main points and conclusions. A set of representative figures, together with extensive descriptive captions, is also included for the reader interested in some additional details. This work was prepared with partial support from various AFGL project orders to NOAA's Space Environment Laboratory during Fiscal Years 1983 through 1985. This support is gratefully acknowledged and reported in each of the 22 papers that are now published, in press, or under consideration in various forums (refereed journals and symposia proceedings).

SUMMARY

The papers listed in the Bibliography are divided into several categories followed by a short description of key points and conclusions.

The four categories are listed as follows:

A. Basic solar wind studies.

B. Magnetohydrodynamic, time-dependent models for the solar wind plasma and interplanetary magnetic field. [short title: MHD Modeling]

C. Coronal mass ejection studies.

D. Technology transfer for geomagnetic storm prediction studies [short title: Technology Transfer]

Some of the main points and conclusions found from the papers included under each category are given in the following sections.

A. Basic Solar Wind Studies

The paper by Cuperman, Tzur, and Dryer (1984) is representative of a series of papers by the group led by Prof. S. Cuperman who has successfully developed a generalization of previously-used, "standard" solar wind equations. This work consists of the derivation-starting from the Boltzmann equation - of a higher order, closed system of equations for the moments of the particle distribution function, f_a for species a, for spherically symmetric systems. This paper uses full equations (rather than the Fourier heat flux expressions) for electron and proton thermal conductivities. A time-dependent, relaxation method is used to obtain steady solutions between the Sun and 5 AU. One of these solutions is shown in Figure 1. The goal of this research is to explore the additional physics, such as dissipative processes, that may become necessary to be incorporated into our 2-1/2D and/or 3D MHD codes when high spatial and temporal resolution may be required. This work is being extended to include electrostatic effects due to unequal proton and electron densities.

In a more operationally-oriented study, Yeh (1984) devised a quantitative model for a corotating solar wind stream. An algorithm was developed for the calculation of the correlation between two points in two disparate streams. Thermal conduction, assuming the commonly-used Fourier heat flux equation for protons only, was assumed to be the main heating along an interplanetary magnetic field (IMF) flux tube.

With the time-dependent magnetohydrodynamic (MHD) models in mind, Yeh and Dryer (1985) developed from first principles a constraint required at the lower boundary in MHD calculations. This constraint is necessary and sufficient for magnetic solenoidality. This is important because numerically-prescribed physical parameters at the lower boundary (say, close to the Sun) can introduce fictitious magnetic monopoles into a medium that was originally free of such monopoles. This constraint, based on Faraday's law, will be incorporated into our MHD modelling work.

B. MHD Modeling

We have followed a very conservative "learning curve" in the construction and testing of our time-dependent computer simulation codes. The modeling has attacked the problem in the classical way: the simultaneous solution of the governing mathematical equations (conservation of mass, momentum, and energy coupled to Maxwell's equations for an electrically-conducting plasma) subject to prescribed initial and boundary conditions. The physics that go into these equations are currently fairly simple: single-fluid electrically neutral, polytropic plasma; no dissipation (except at shocks); and gravitational attraction by the Sun. Additional physics has been developed in a parallel track as mentioned in Section A above and in the papers given in the Bibliography (as well as in various review papers by participants in this project: M. Dryer, S. Cuperman, and S.T. Wu). Such additional physics will be incorporated into future extensions of our models.

We have continued to utilize the computers available to us, starting with CDC 6600, then moving to the CDC 7600, followed by CYBER's 650, 750, and now

the CYBER 840 (all in Boulder). In addition, we have utilized the CRAY-1 (NCAR/Boulder) and, now, the CYBER 855/205 (NOAA/NBS/Gaithersburg, MD). Developmental work is also currently being accomplished on an APOLLO microcomputer. An NCAR graphics package, together with several routines of our own design, has been helpful. Additional machines (PDP VAX and UNIVAC) have also been used by several of our contractors (Tennessee Technological University and Engineering International, Inc.) as part of our focused study.

With the physics and mathematics combined and with the usage of the computers, we have utilized the approach of the initial boundary value problem of mathematical physics. That is, with initial configurations as specified above, various lower boundary conditions have been imposed to generate the disturbances. These lower boundary conditions are chosen to simulate a variety of solar conditions, such as flares, prominence eruptions, coronal mass ejections, etc. Figures 2, 3, and 4, together with their captions, illustrate some of our basic studies with the 2-1/2D MHD model. Sensitivity studies with varying pulse strengths and durations are given in the Bibliography. As time progresses, we hope that the evolutionary plasma properties will reflect reality as closely as possible. The need for observational comparisons is obvious, and we have indeed made several comparisons of this kind. One must keep in mind that no analytic solutions are available for the problems that confront us, namely varying conditions at the Sun that cause compound evolutionary changes in an inhomogeneous steady-state heliospheric medium. A single caveat should be stated: use of similarity theory has proved useful and instructive in simple situations such as the blast wave and constant velocity piston-driven cases.

The question of geometry is important. We obviously must live in a three-dimensional universe. But insight must come along the "learning curve" by progressing from one to two, then to three dimensional, time-dependent simulations. We have followed this course and have now achieved the fully-3D stage. However, we continue, on occasion, to fall back on the 2D, 2-1/2D (three components of IMF and solar wind velocity are considered on the ecliptic plane), and even the 1-1/2D (two components along a fixed helioradial direction) models. This approach is essential whenever we have found complete sets of data from two radially-aligned spacecraft or from widely-separated spacecraft within (or close to) the ecliptic plane. We have successfully completed the former case (1-1/2D solution with Pioneer 10 and 11 spacecraft) as indicated by Smith, Dryer, and Steinolfson (1984a, and references therein).

Most of our work has been done in the 2D and 2-1/2D area with the simulation of solar flare shocks, high-speed coronal hole streams, and combinations of these forms of solar activity. The latter work is described by Dryer and Smith (1986) and Dryer et al. (1986) who attempted to simulate the interplanetary response to more than 10 days of substantial activity on the Sun during STIP Interval VII (August 1979); the results were mixed. Figures 5, 6, 7, and 8 are representative of this study of a series of an eruptive prominence that was superimposed on a low-speed stream that was bracketed by higher-speed coronal hole streams. The figures, supported by the material in the figure captions, will give the interested reader the flavor for the simulated response in the ecliptic plane as well as at Earth (actually, ISEE-3) following a series of five solar flares, several of which

were followed by coronal mass ejections that were observed by P78-1's SOLWIND coronagraph. We gained a greater respect for the need to observe and analyze the solar and near-sun conditions needed to drive the model. A study of isolated solar flare shocks was made by Dryer et al. (1984) to demonstrate the model's use as a prediction module for prediction of solar wind "geoeffective" parameters, ε and VB_z. A time series of one such example is shown in Figure 9 for three hypothetical locations of Earth relative to a single solar flare-generated shock wave. Improvements to the numerical algorithm are described by Han et al. (1984b). The influence of a pre-exiting inhomogeneity in the solar wind on a flare-generated shock wave response in the interplanetary medium was studied by Gislason et al. (1984). The pre-existing inhomogeneity was found by simulating an equatorially-fluctuating heliospheric current sheet. A review of some of this work is given by Dryer (1984) who also discussed the pioneering aspects of our 3D work.

One of our studies (Smith, Dryer, and Han, 1985b) was directed to a question frequently asked by forecasters: given a series of solar events, such as flares and/or disappearing filaments, why do some of them have geophysical consequences and the others do not? Figure 10 illustrates a case of interplanetary pressure contours produced by a series of three individual pulses. The first one produces a forward shock wave that, presumably, would produce a SSC if Earth were located along any of their radial rays labeled 1-5. The second one, however, produces a shock that is strongly attenuated by its interactions with the disturbed flow in their wake of the first shock. Hence, in this scenario, the Earth (at any of the radial rays, 1-5) would not experience a SSC from the second pulse. Indeed, even a third pulse (see T=30 hr. in Figure 10) produces a shock that is also strongly attenuated by the time of its arrival twenty hours later, particularly at 1 AU along ray paths 1 and 5.

Moving into the 3D area has highlighted the need for the supercomputer (CRAY-1 and/or CYBER 855/205). We have considered to date a computational domain from 18 solar radii (0.08 AU) to 1.1 AU in the helioradial direction and 90° in both the heliolongitudinal and heliolatitudinal directions, the latter being 45° on each side of the solar ecliptic plane. In keeping with our conservative approach, both scientifically and from a computer usage viewpoint, we have studied thus far a single shock whose central axis is located in the ecliptic plane. Figures 11, 12, and 13 show some of the results of this work that was performed on the CRAY-1. The outer limit for this simulation was 76 solar radii when these figures were prepared but has since been extented to 1.2 AU for this $90^\circ \times 90^\circ$ solid angle, the lower half of which is symmetrical to the upper half. In this first case, we have as yet not utilized the capability of the southern hemispherical domain. The basic study is described in detail by Han et al. (1984a) and by Han, Wu, and Dryer (1986); shorter summaries are given by Dryer (1984) and by Dryer, Wu, and Han (1986) for the earlier and most recent results, respectively. A major new feature is the large-scale twisting of the IMF, a discovery that may be relevant to the "magnetic cloud" observations as well as to future forecasting algorithms.

C. Coronal Mass Ejection Studies

Magnetic stresses have been proposed as one of the physical mechanisms that drive coronal loops, such as prominences, away from the Sun. Yeh (1985) has described these stresses in the more general context of hydromagnetic buoyancy. This paper provides the mathematical explanation in a detail not covered by earlier proponents of the so-called "magnetically-driven" coronal mass ejections (CMEs).

A complementary description of the CME phenomenon has been proposed by our group. We have suggested the use of MHD modeling as a tool for understanding the coronal response to an arbitrarily-prescribed input at the coronal base. Thus far, our models have been in the 2D and 2-1/2D mode only as part of our fundamental approach toward a 3D capability. Some of our early results (circa 1977-78) has been criticized by several experimenters. Our comments on their work are given by Dryer and Wu (1985) who pointed to the authors' bias in their choice of a limited, white-light, data sample and their neglect of our other numerical results in arriving at their conclusions about their observation/model study.

We have also continued our collaboration with a large group of observers of coronal transients for specific cases. Some of this work is given by Harrison et al. (1985) and Maxwell, Dryer, and McIntosh (1985). This work demonstrates the acceptance of our MHD modeling by a larger group of observers who have considered many diagnostics (radio, H-alpha, X-ray images, and *in situ* spacecraft data) in addition to white-light imagery.

D. Technology Transfer

Work by Air Force Geophysical Laboratory scientists in the area of flare shocks' times-of-arrival at Earth has stimulated several possible extensions as proposed by Pinter and Dryer (1985a, b). These suggest that the Type IV diagnostic feature may be relevant to the piston-driven phase of a flare-generated shock. That is, the duration of this radio emission for the most energetic flares might be used in place of the soft X-ray duration. They also suggested that the integrated energy flux in the soft X-rays (say, 1-4Å) could be correlated with the flare energy output and the time for the shock to reach Earth. A summary result of this work on the average kinematic property of flare-generated shocks is given in Figure 14 with additional details provided in the figure caption.

A much more general study has been developed for the transfer of verified research into an operationally-oriented forecast strategy. This work by Dryer et al. (1985) is aimed toward development of a "solar-terrestrial environment model" as a key strategic element for an operational geomagnetic storm forecasting tool for the late 1990s when operational SIMPL and SAMSAT spacecraft could provide more solar corona and solar wind data to drive MHD models. The strategy is clearly 3D-oriented with photospheric, coronal, interplanetary, magnetospheric, ionospheric, thermospheric, and even neutral atmosphere models as individual modules placed end-to-end. An example computation is given from the photosphere to the auroral ionosphere (following a coronal mass ejection that is preceded by a shock) by Wu, Dryer, and Han

(1985). We have decided to call this global concept STEM-2000, with the hope that all elements will be in place by that date. This concept, or strategy, is outlined in Figure 15 (and its caption) in several block diagram formats, the upper half relative to the sun/interplanetary connections and the lower half relative to the interplanetary/magnetosphere/ionosphere connections. Clearly, a further connection (not shown here) should be made to the thermosphere and its coupling to the neutral atmosphere.

CONCLUDING REMARKS

This Final Report consists of a brief outline of the work described in 22 publications. The scope of work is suggested in four major categories: (a) basic solar wind studies, (b) MHD modeling, (c) coronal mass ejections, and (d) technology transfer that is oriented to the national goal of achieving long range predictions of geomagnetic storms.

BIBLIOGRAPHY

Cuperman, S., I. Tzur, and M. Dryer, Numerical Investigation of Fluid Models with Full Electron and Proton Thermal Conduction Equations for the Quiet Solar Wind, Astrophys. J., 286, 763-771, 1984.

Dryer, M., S.T. Wu, G. Gislason, S.M. Han, Z.K. Smith, J.F. Wang, D.F. Smart, and M.A. Shea, Magnetohydrodynamic Modelling of Interplanetary Disturbances Between the Sun and Earth, Astrophys. Space Sci., 105, 187-208, 1984.

Dryer, M., Examples of Two-and Three-Dimensional Time-Dependent Simulation of Solar Flare Generated Shock Waves, in Extended Abstracts of Joint U.S. - Japan Seminar on the Heliomagnetosphere, pp. 87-93, November 5-9, 1984.

Dryer, M. and S.T. Wu, Comments on "Density Distributions in Looplike Coronal Transients: A Comparison of Observations and a Theoretical Model" by D.G. Sime, R.M. MacQueen, and A.J. Hundhausen, J. Geophys. Res., 90, 559-561, 1985.

Dryer, M., S.-I. Akasofu, H.W. Kroehl, R. Sagalyn, S.T. Wu, T.F. Tascione, and Y. Kamide, The Solar/Interplanetary/Magnetosphere/Ionosphere Connection: A Strategy for Prediction of Geomagnetic Storms, AAS/AIAA Astrodynamics Specialist Conference; Vail, Colorado, Preprint AAS/AIAA 85-313, August 12-15, 1985, J. Astrodyn. Sci., submitted, 1985.

Dryer, M., Z.K. Smith, S.T. Wu, S.M. Han, and T. Yeh, MHD Simulation of the "Geoeffectiveness" of Interplanetary Disturbances, in AGU Chapman Conference in Solar Wind-Magnetosphere Coupling (Y. Kamide and J. A. Slavin, Eds.), Terra Scientific Publ. Co., Tokyo, in press, 1986.

Dryer, M., S.T. Wu, and S.M. Han, Three-Dimensional, Time-Dependent, MHD Model of a Solar Flare-Generated Interplanetary Shock Wave, in 19th ESLAB Symposium on the Sun and the Heliosphere in Three Dimensions, June 4-6, 1985, Les Diablerets, Switzerland, (K.-P. Wenzel and R.G. Marsden, Eds.), D. Reidel Publ. Co., Dordrecht, in press, 1986.

Dryer, M. and Z.K. Smith, MHD Simulation of Multiple Interplanetary Disturbances During STIP Interval VII (August 1979), Proceedings of Solar Maximum Analysis Symposium, (V.E. Stepanov and V. Obridko, Eds.) VNU Science Press BV, Utrecht, The Netherlands, in press, 1986.

Gislason, G., M. Dryer, Z.K. Smith, S.T. Wu, and S.M. Han, Interplanetary Disturbances Produced by a Simulated Solar Flare and Equatorially-Fluctuating Heliospheric Current Sheet, Astrophys. Space Sci., 98, 149-161, 1984.

Han, S.M., S. Panitchob, S.T. Wu, and M. Dryer, A Numerical Simulation of Three-Dimensional Transient Ideal Magnetohydrodynamic Flows, Proceedings of Southeastern Conference on Theoretical and Applied Mechanics XII, Callaway Gardens, GA, May 10-11, 1984, Volume II, pp. 39-45, Auburn University, Engineering Extension Service, 1984a.

Han, S.M., S.T. Wu, Z.K. Smith, and M. Dryer, Numerical Study of Two-Dimensional Non-Plane MHD Wave Propagation in a Supersonic, Superalfvenic, Magnetohydrodynamic Flow, AIAA 17th Fluid Dynamics, Plasma Dynamics, and Lasers Conference, Snowmass, CO, June 25-27, 1984, Preprint No. AIAA-84-1598; 1984b.

Han, S.M., S.T. Wu, and M. Dryer, A Transient, Three-Dimensional MHD Model for Numerical Simulation of Interplanetary Disturbances, in STIP Symposium on Retrospective Analyses and Future Coordinated Intervals, 10-12 June 1985, Les Diablerets, Switzerland, (M.A. Shea, D.F. Smart, Eds.), Book Crafters Publ. Co., Chelsea, MI, in press, 1986.

Harrison, R.A., P.W. Waggett, R.D. Bentley, K.J.H. Phillips, M. Bruner, M. Dryer, and G.M. Simnett, The X-Ray Signature of Solar Coronal Mass Ejections, Solar Phys., in press, 1985.

Maxwell, A., M. Dryer, and P.S. McIntosh, A Piston-Driven Shock in the Solar Corona, Solar Phys., in press, 1985.

Pinter, S. and M. Dryer, The Influence of the Energy Emitted by Solar Flare Soft X-Ray Bursts on the Propagation of Their Associated Interplanetary Shock Waves, Astrophys. Space Sci., in press, 1985a.

Pinter, S. and M. Dryer, Conversion of Piston-Driven Shocks from Powerful Solar Flares to Blast Wave Shocks in the Solar Wind, Solar Phys., submitted, 1985b.

Smith, Z.K., M. Dryer, and R.S. Steinolfson, A Study of the Formation, Evolution and Decay of Shocks in the Heliosphere Between 0.5 and 30.0 AU, J. Geophys. Res., 90, 217-220, 1985a.

Smith, Z.K., M. Dryer, and S.M. Han, Interplanetary Shock Collisions: Forward with Reverse Shocks, Astrophys. Space Sci., in press, 1985b.

Wu, S.T., M. Dryer, and S.M. Han, The Solar Flare-Induced Earth's Environment, AAS/AIAA Astrodynamics Specialist Conference, Vail, Colorado, Preprint AAS 85-314, August 12-15, 1985, J. Astrodyn. Sci., submitted, 1985.

Yeh, T., A Hydrodynamic Model of Corotating Conductive Solar Wind Streams, Astrophys. Space Sci., 98, 353-366, 1984.

Yeh, T., Hydromagnetic Buoyancy Force in the Solar Atmosphere, Solar Phys., 95, 83-97, 1985.

Yeh, T., and M. Dryer, A Constraint on Boundary Data for Magnetic Solenoidality in MHD Calculations, Astrophys. Space Sci., in press, 1985.

FIGURE CAPTIONS

Figure 1 Two-fluid, steady-state, solar wind solution with full equations (rather than Fourier heat flux expressions) for electron and proton thermal conductivities using higher order, closed system of equations starting from the Boltzmann equations. The streaming velocity, density (assumed: $n = n_p = n_e$), temperature, and electron heat flux distributions are shown above as a function of heliocentric distance in solar radii. The lower plot shows the various contributions to the total energy flux. (Cuperman, Tzur, and Dryer, 1984).

Figure 2 Typical homogeneous solar wind velocity profile (i.e., independent of heliolongitude) in the ecliptic plane. It is essential in MHD simulations research that the pre-disturbed condition (represented by velocity maps such as this one) be recovered after the effects of simulated disturbances move to distances beyond 1 AU. (Dryer et al., 1984)

Figure 3 Temporal and spatial solar wind velocity dispersion produced by a strong solar flare-generated shock wave as viewed in the ecliptic plane. Figure 3(a) - 3(d) show the vector change, with maximum increases as indicated, as time increases from t = 20.2 hr to t = 80.2 hr. Note that the ΔV decreases with time as the disturbance propagates beyond 1 AU.

Figure 4 Fractional density changes in the ecliptic plane for the same case shown in Figure 3. The maximum initial shock velocity in the simulation is taken to be V_s = 3000 km sec^{-1} along the central (vertical) axis with a sinusoidal decrease to zero at $\pm 12^o$ of this axis. This approximation to a non-spherical shock is applied near the sun (18 solar radii) for a period of 5400 sec to simulate a finite duration of flare energy output rate. The half-tone presentation demonstrates both compression and rarefaction, followed by a numerically-acceptable return to ambient conditions after the shocked disturbances passes out of the 1.2 AU circular computational domain.

Figure 5 Representative solar wind response to a series of simulated coronal hole streams followed by an eruptive prominence during STIP Interval VII (August 1979). As in Figure 2, the vertical dimension represents the total solar wind velocity within a 150^o range of ecliptic heliolongitudes. The time shown (T = 140.1 hr) is elapsed time since T = 0 hr as simulated in this 2-1/2D MHD model since 0 hr on 8 August 1979. (Dryer et al, 1986).

Figure 6 Simulated unit vectors of the interplanetary magnetic field (IMF) at T = 160 hr during the simulation of the compounded, multiple events in August 1979. (Dryer et al., 1986).

Figure 7 Simulated solar wind velocity (center panel) at Earth's location for the multiple events in August 1979. The lowest panel shows the simulation for a nine-day period under the assumptions that there were no solar disturbances other than a series of the three corotating solar wind streams, two moderately-high ones that led and followed a lower speed stream. The upper panel shows the ISEE-3 observations.

Figure 8 Simulated IMF magnitude (center panel) at Earth's location for the multiple events in August 1979 (see, also, Figure 7). The ISEE-3 observations, when compared to the simulated ones demonstrate the need for improved observational requirements for driving the model close to the sun as well as improvements to the physics and numerical procedures (grid size, for example) for the model.

Figure 9 Illustration of the temporal series of several proposed indices (ε and $VB_{\perp}$ [or VB_z]) at 1 AU. Three possible locations of Earth relative to a representative, single, solar-flare-generated shock disturbance are shown in this example.

Figure 10 Total pressure contours (logarithm of the thermal plus magnetic pressures) in the ecliptic plane following a series of three separate assumed solar disturbances. The responses detected by hypothetical observers along the heliocentric ray paths labeled 1-5 are all different. They depend upon the spatial locations and strengths of each individual solar pulse. Strong attenuation can occur; for example, at $15 < T < 30$ hr, the interplanetary MHD shock wave from the second pulse is nearly completely dissipated by its interactions with the reverse MHD shock from the first pulse. (Z. Smith, Dryer, and Han, 1985b)

Figure 11 Three-dimensional deformation of the interplanetary magnetic field (IMF) caused by a single solar flare-generated shock wave. Left side of the figure shows the ecliptic plane projections of the IMF; the MHD shock at times of 5 and 10 hr can be discerned where the Archimedian spiral is initially distorted. The leading shock has moved outside of the outer limit, 76 solar radii, of this display at 20 hr and has nearly returned to its original spiral at 30 hr. Right side of the figure shows a meridional "cut" at latitudes from ± 45 through the center of the left-side display. The outward, bubble-like deformations of the IMF is caused by a large amplitude nonlinear Alfven wave behind the leading fast mode MHD shock. (Han et al., 1984a; Dryer, Wu, and Han, 1986)

Figure 12 Three-dimensional model simulation of changes in the solar wind at 32 solar radii following a solar-flare shock wave that was generated 5 hrs. earlier. The top two panels show the near-doubling of the radial solar wind velocity within a 90° longitudinal sector. The center panels show the transverse components of the disturbed solar wind velocity. The lower panels show the magnitudes of the IMF. (Han et al., 1984a; Dryer, Wu, and Han, 1986).

Figure 13 Three-dimensional model simulation of the plasma density changes at several heliocentric radial locations and at several times following the outward progression of a single solar flare-generated shock wave. Development of a secondary, annular density maximum (the first being at the MHD forward shock itself) is clearly seen. It is believed that this internal maximum represents development of a MHD reverse shock. (Han et al., 1984a; Dryer, Wu, and Han, 1986).

Figure 14 Empirically-derived average characteristic velocity profile of flare-generated interplanetary shock waves as based on a sample of 39 cases. This presentation, based on a model developed at the Air Force Geophysics Laboratory, approximates an initially constant velocity piston-driven shock, followed by a decelerating "blast" shock that is convected by the background solar wind plasma. In the average case, a shock is driven at its Type II-determined velocity of 1560 km sec^{-1} to a distance of 0.12 AU during a time suggested by the duration of the soft X-ray or Type IV event. Following this "flare duration" or "piston driving time", the shock decelerates to 540 km sec^{-1} (at 0.837 AU) convected by an average background solar wind velocity of 300 km sec^{-1}. The blast wave's average velocity, then, is 890 km sec^{-1} from the end of its driven phase. This average characteristic is based on the 39 cases that had a wide range of shock shapes and flare locations relative to Earth. (Pinter and Dryer, 1985b).

Figure 15 Block diagram illustrating a physically-based strategy for the predictions of geomagnetic storms: whether and when it will occur, how long it will last, and how severe it will be. The upper half of the figure is limited to the solar and interplanetary portion of the physical linkage: real time observations from the SOON/RSTN sites plus satellites (GOES-NEXT, SAMSAT) would provide input parameters that will drive MHD models of the photospheric, chromospheric, and coronal dynamics under both quiet and active conditions. The outputs of these models then feed into MHD solar wind codes that output basic geoeffective physical parameters such as dynamic pressure, Poynting power flux, and cross tail electric field from the solar wind velocity, density, and IMF parameters. The lower half of the figure indicates the need for "ISEE-3 type" of upwind real-time monitoring by a Synoptic Interplanetary Monitoring Platform (SIMPL) which would be required for updating the MHD solar wind "interplanetary global circulations model." The solar wind parameters, thus determined, are used via statistical studies incorporated into a kinematic code to determine predictions of the polar cap and auroral zone boundaries and, if desired, the geomagnetic and auroral electrojet indices as well as the ionospheric current and electrical conductivity distributions. Meanwhile, real-time ground-based magnetometer variations, ionospheric observations, AF/DMSP and NOAA/TIROS data are used as inputs for additional models of magnetosphere-ionosphere coupling processes (KRM, "Polar") to determine Joule heat, electron density profiles, and probable locations for satellite drag increases. (Dryer, et al., 1985).

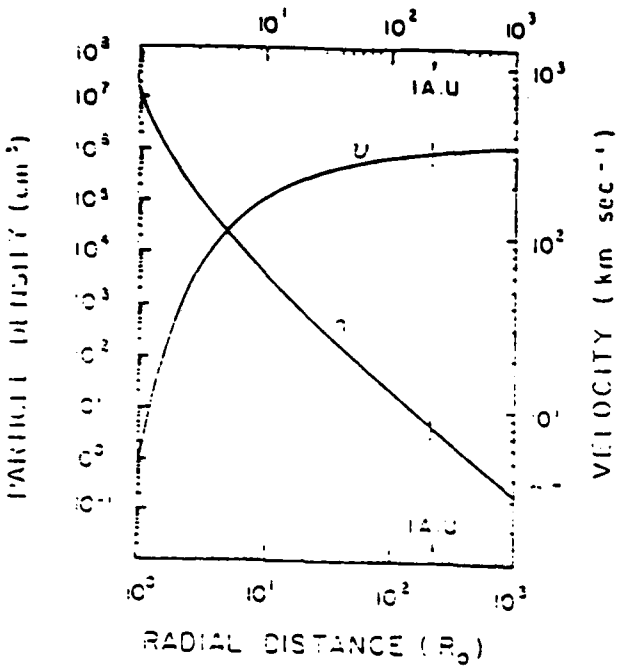
1A.U
U
1A.U
VELOCITY (km sec⁻¹)
RADIAL DISTANCE (R₀)

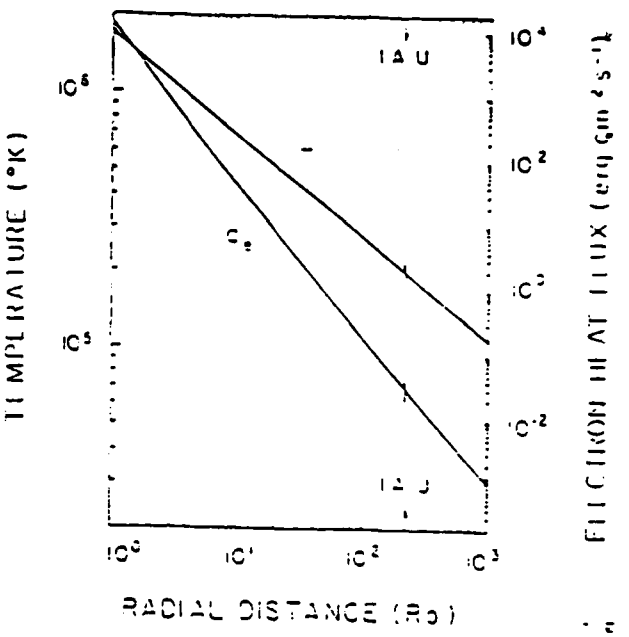
1A.U
1A.U
RADIAL DISTANCE (R₀)

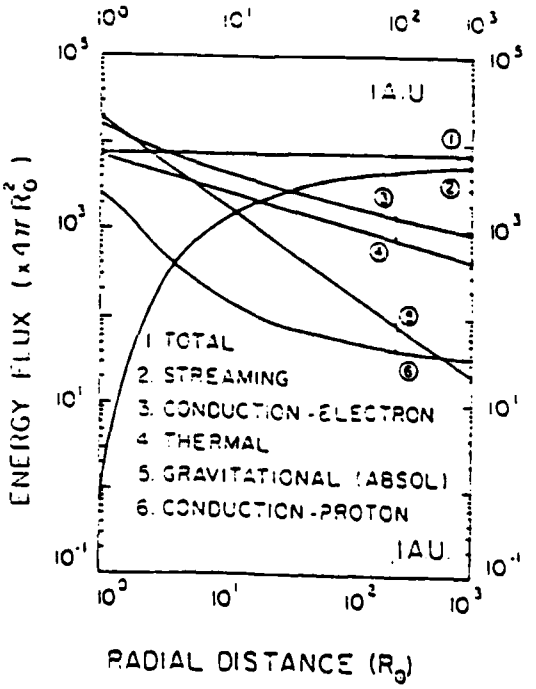
1A.U
1. TOTAL
2. STREAMING
3. CONDUCTION - ELECTRON
4. THERMAL
5. GRAVITATIONAL (ABSOL)
6. CONDUCTION - PROTON
1A.U.
ENERGY FLUX
RADIAL DISTANCE (R₀)

Figure 1.

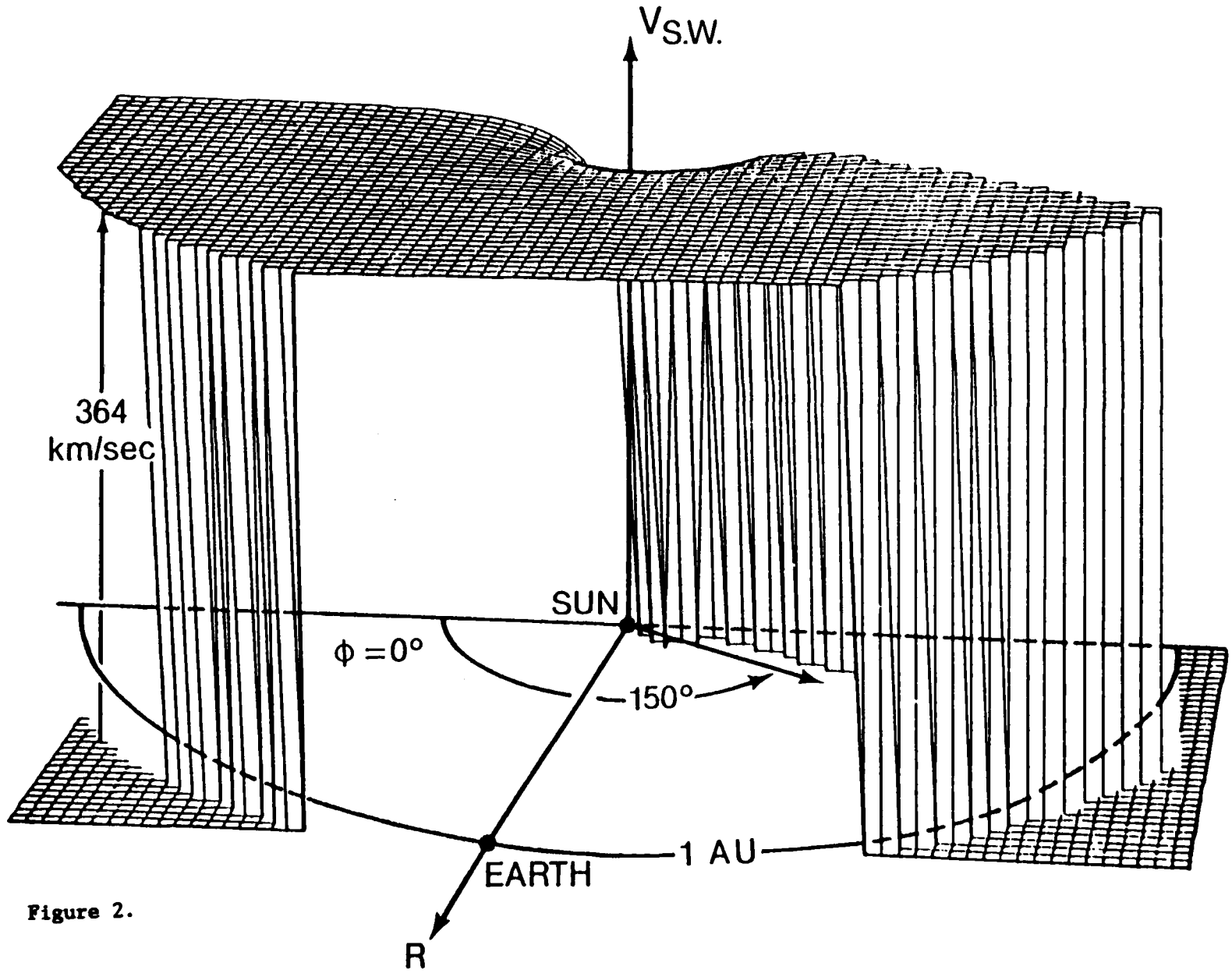
T=0.0 HOURS
VELOCITY SURFACE
$V_{S.W.}$
364
km/sec
SUN
$\phi = 0°$
150°
1 AU
EARTH
R

Figure 2.

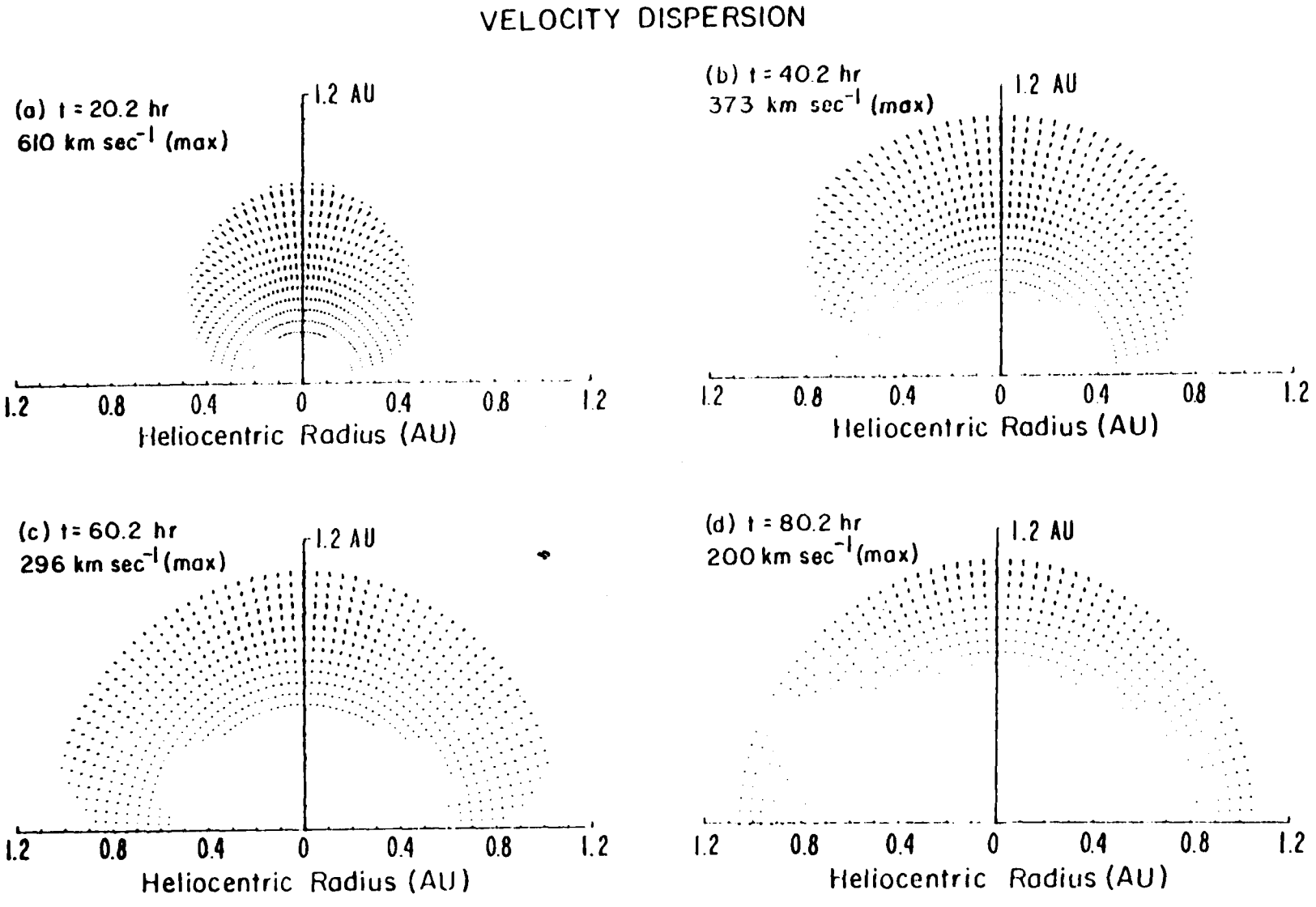
VELOCITY DISPERSION
(a) t = 20.2 hr
610 km sec^{-1} (max)
1.2 AU
1.2 0.8 0.4 0 0.4 0.8 1.2
Heliocentric Radius (AU)
(b) t = 40.2 hr
373 km sec^{-1} (max)
1.2 AU
1.2 0.8 0.4 0 0.4 0.8 1.2
Heliocentric Radius (AU)
(c) t = 60.2 hr
296 km sec^{-1} (max)
1.2 AU
1.2 0.8 0.4 0 0.4 0.8 1.2
Heliocentric Radius (AU)
(d) t = 80.2 hr
200 km sec^{-1} (max)
1.2 AU
1.2 0.8 0.4 0 0.4 0.8 1.2
Heliocentric Radius (AU)

Figure 3.

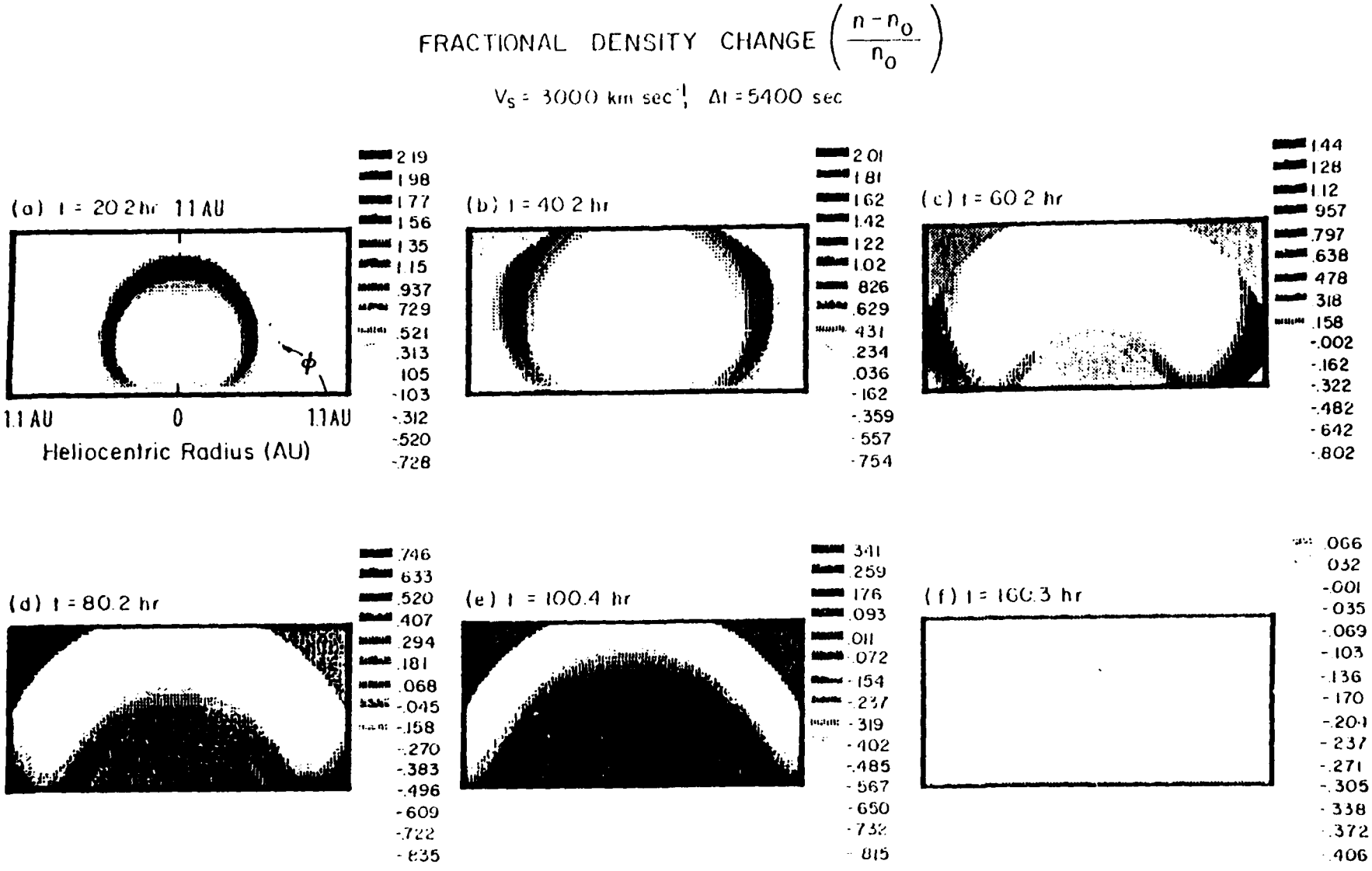
FRACTIONAL DENSITY CHANGE $\left(\frac{n-n_0}{n_0}\right)$
V_S = 3000 km sec^{-1}, Δt = 5400 sec
(a) t = 20.2 hr 1.1 AU
(b) t = 40.2 hr
(c) t = 60.2 hr
(d) t = 80.2 hr
(e) t = 100.4 hr
(f) t = 160.3 hr
1.1 AU
0
1.1 AU
Heliocentric Radius (AU)
2.19 1.98 1.77 1.56 1.35 1.15 .937 .729 .521 .313 .105 -.103 -.312 -.520 -.728
2.01 1.81 1.62 1.42 1.22 1.02 .826 .629 .431 .234 .036 -.162 -.359 -.557 -.754
1.44 1.28 1.12 .957 .797 .638 .478 .318 .158 -.002 -.162 -.322 -.482 -.642 -.802
.746 .633 .520 .407 .294 .181 .068 -.045 -.158 -.270 -.383 -.496 -.609 -.722 -.835
.341 .259 .176 .093 .011 -.072 -.154 -.237 -.319 -.402 -.485 -.567 -.650 -.732 -.815
.066 .032 -.001 -.035 -.069 -.103 -.136 -.170 -.204 -.237 -.271 -.305 -.338 -.372 -.406

Figure 4.

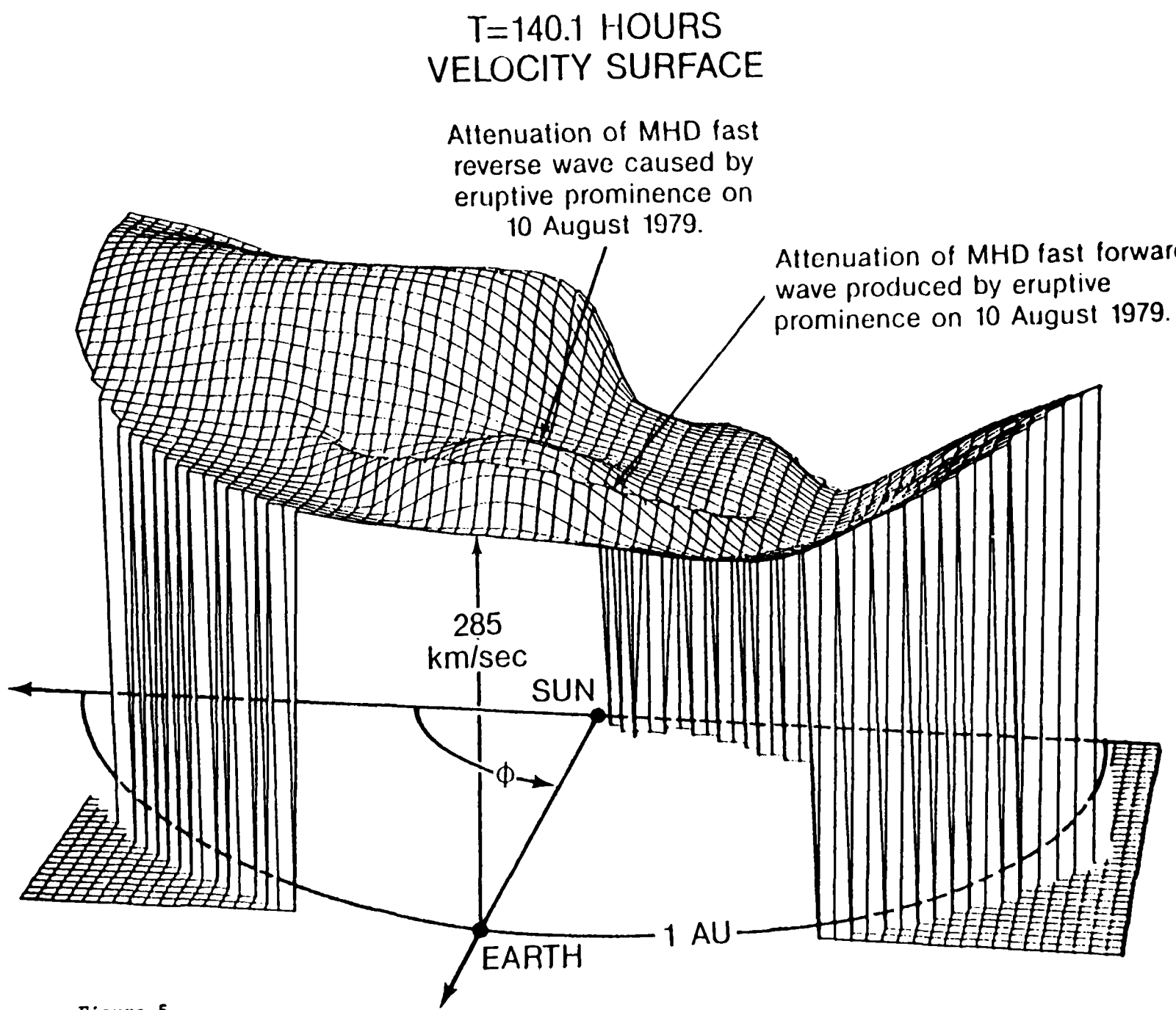
T=140.1 HOURS
VELOCITY SURFACE
Attenuation of MHD fast reverse wave caused by eruptive prominence on 10 August 1979.
Attenuation of MHD fast forward wave produced by eruptive prominence on 10 August 1979.
285 km/sec
SUN
ϕ
1 AU
EARTH
R

Figure 5.

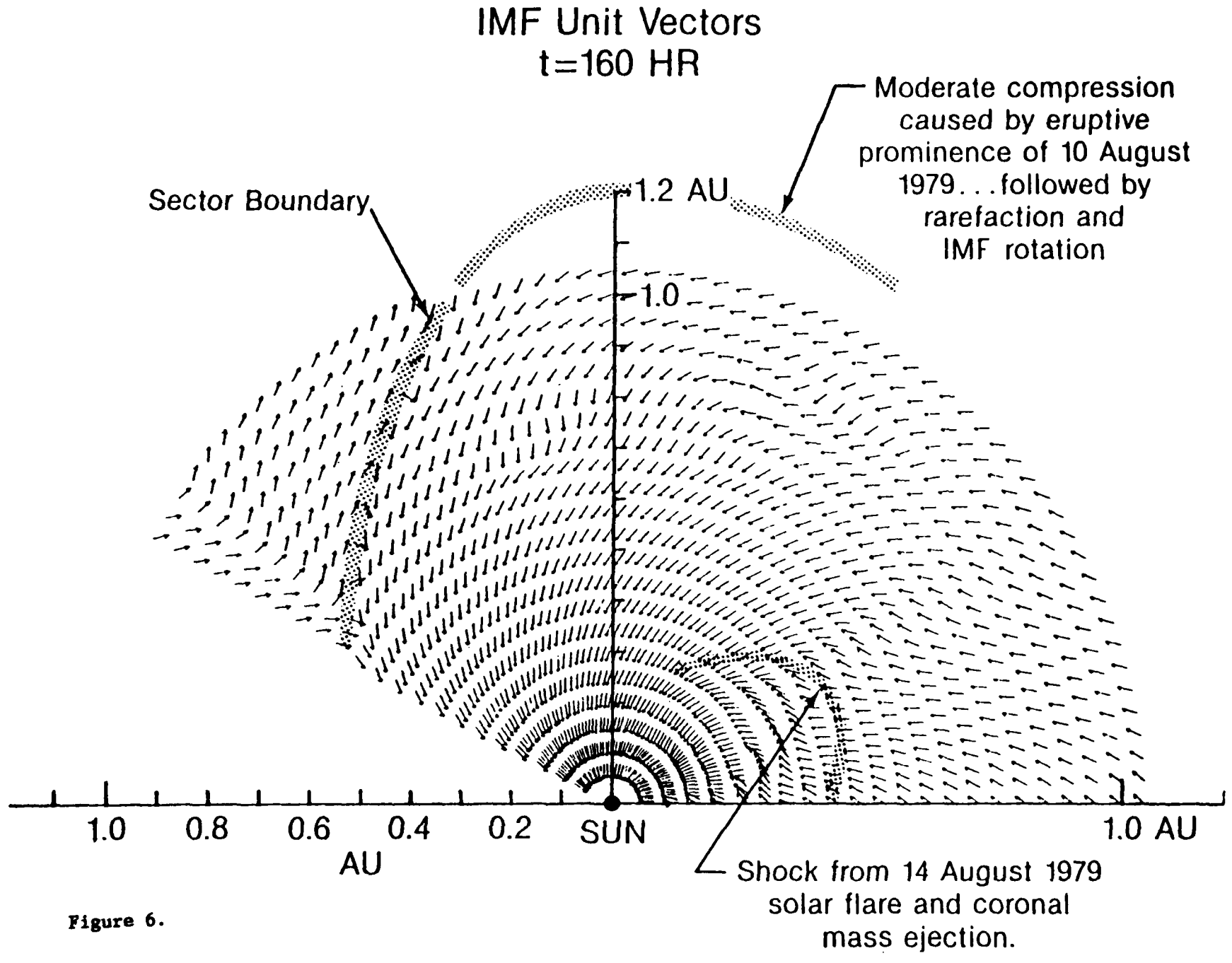
IMF Unit Vectors
t=160 HR
Moderate compression caused by eruptive prominence of 10 August 1979...followed by rarefaction and IMF rotation
Sector Boundary
1.2 AU
1.0
1.0
0.8
0.6
0.4
0.2
SUN
1.0 AU
AU
Shock from 14 August 1979 solar flare and coronal mass ejection.

Figure 6.

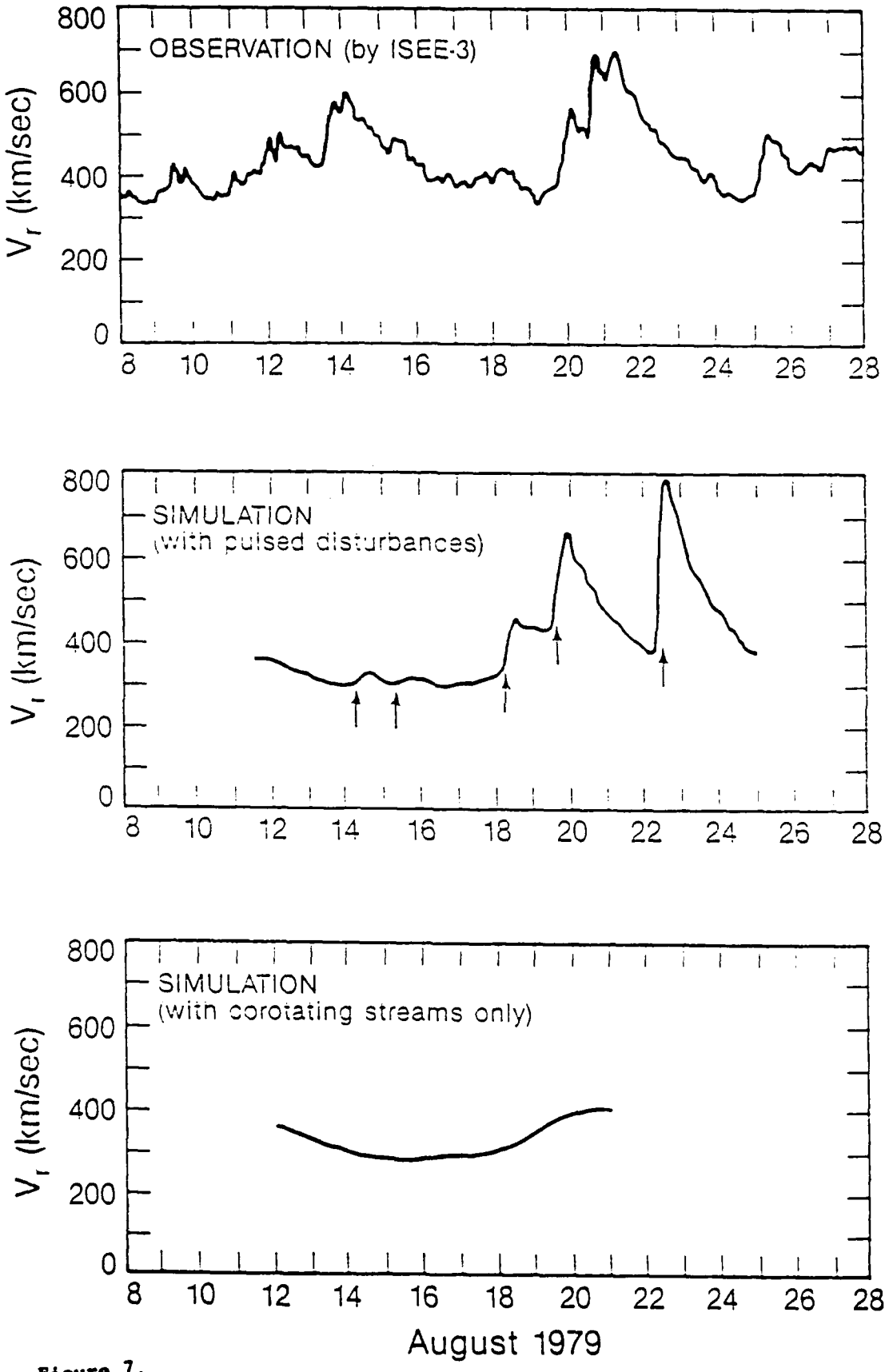
OBSERVATION (by ISEE-3)
SIMULATION
(with pulsed disturbances)
SIMULATION
(with corotating streams only)
V_r (km/sec)
800
600
400
200
0
8
10
12
14
16
18
20
22
24
26
28
August 1979

Figure 7.

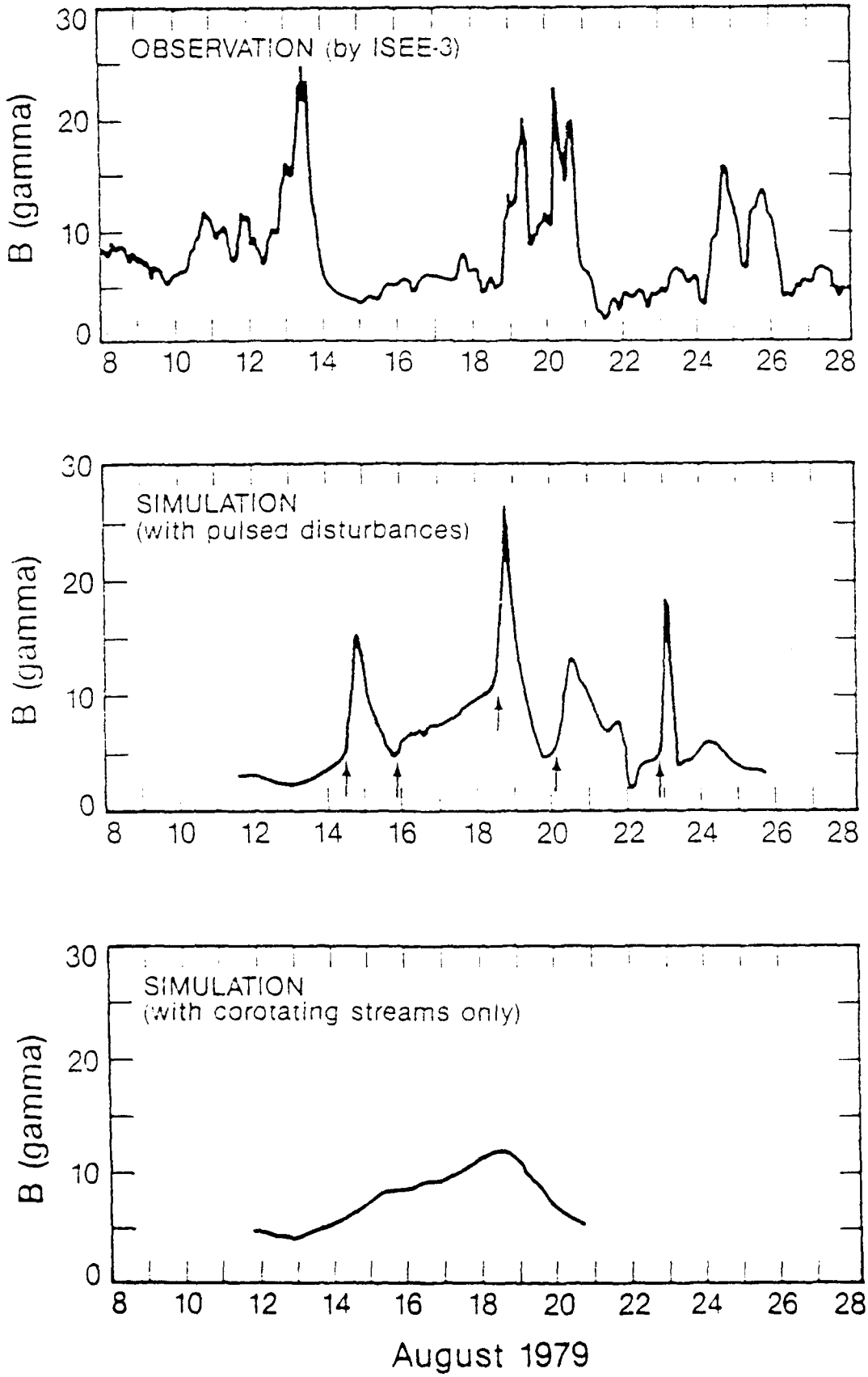
OBSERVATION (by ISEE-3)
SIMULATION
(with pulsed disturbances)
SIMULATION
(with corotating streams only)
B (gamma)
0
10
20
30
8
10
12
14
16
18
20
22
24
26
28
August 1979

Figure 8.

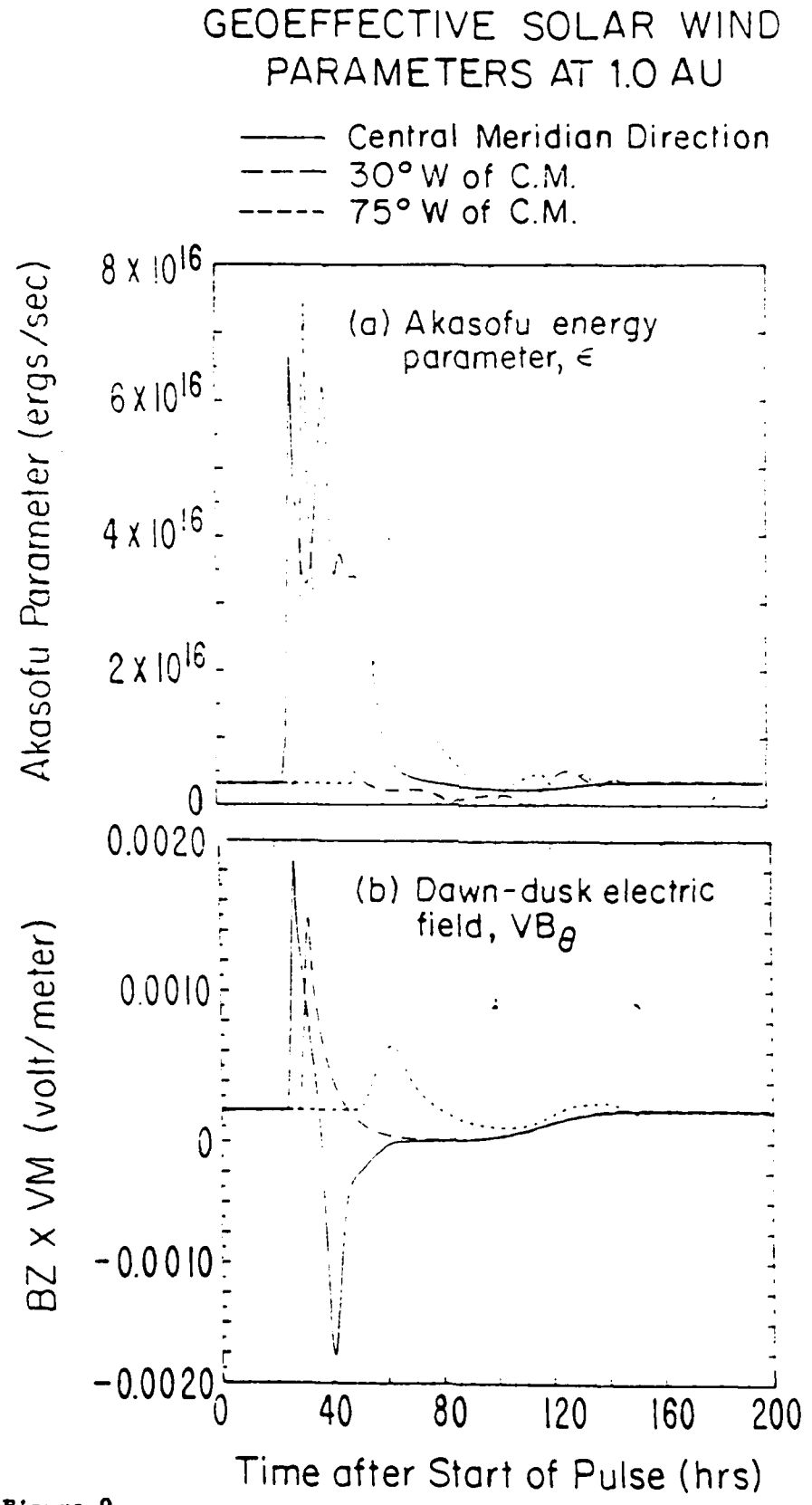

Figure 9.

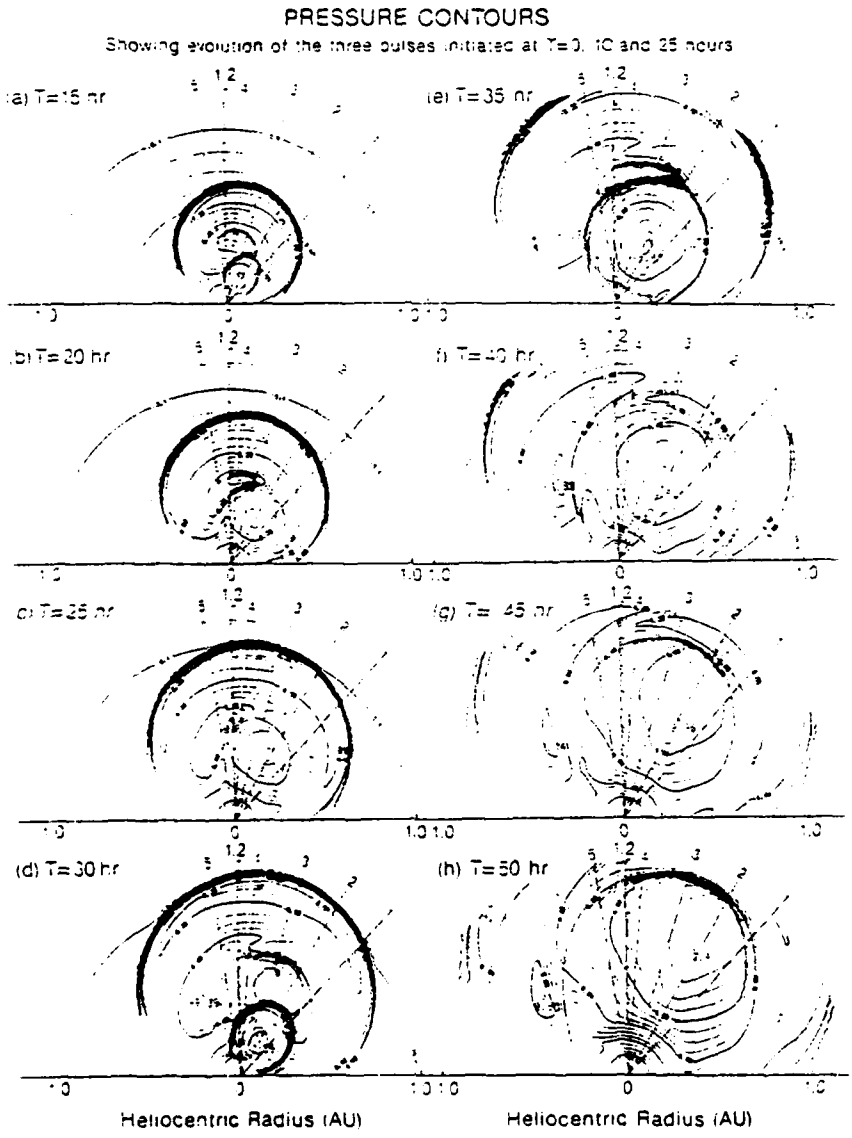

Figure 10.

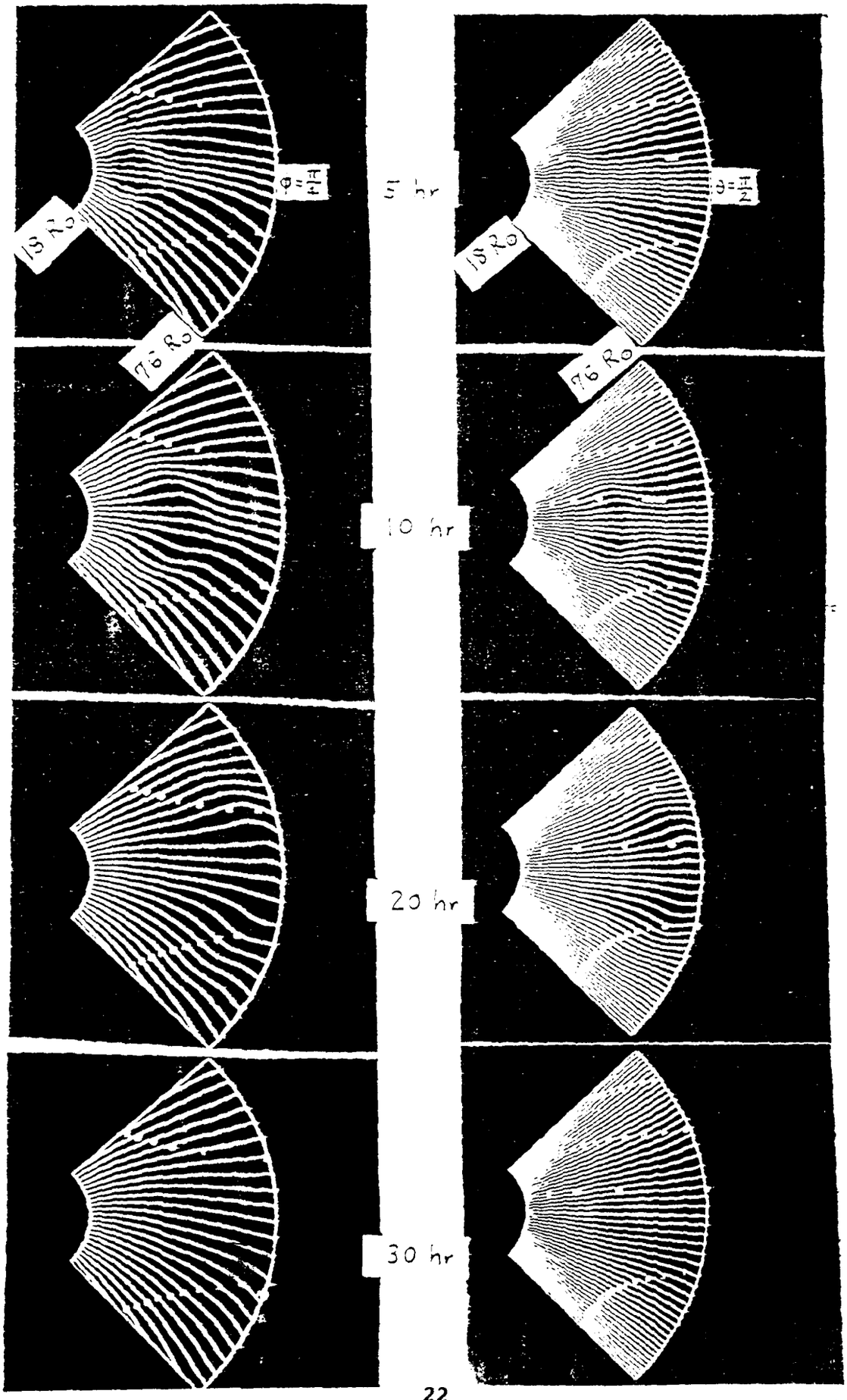

Figure 11.

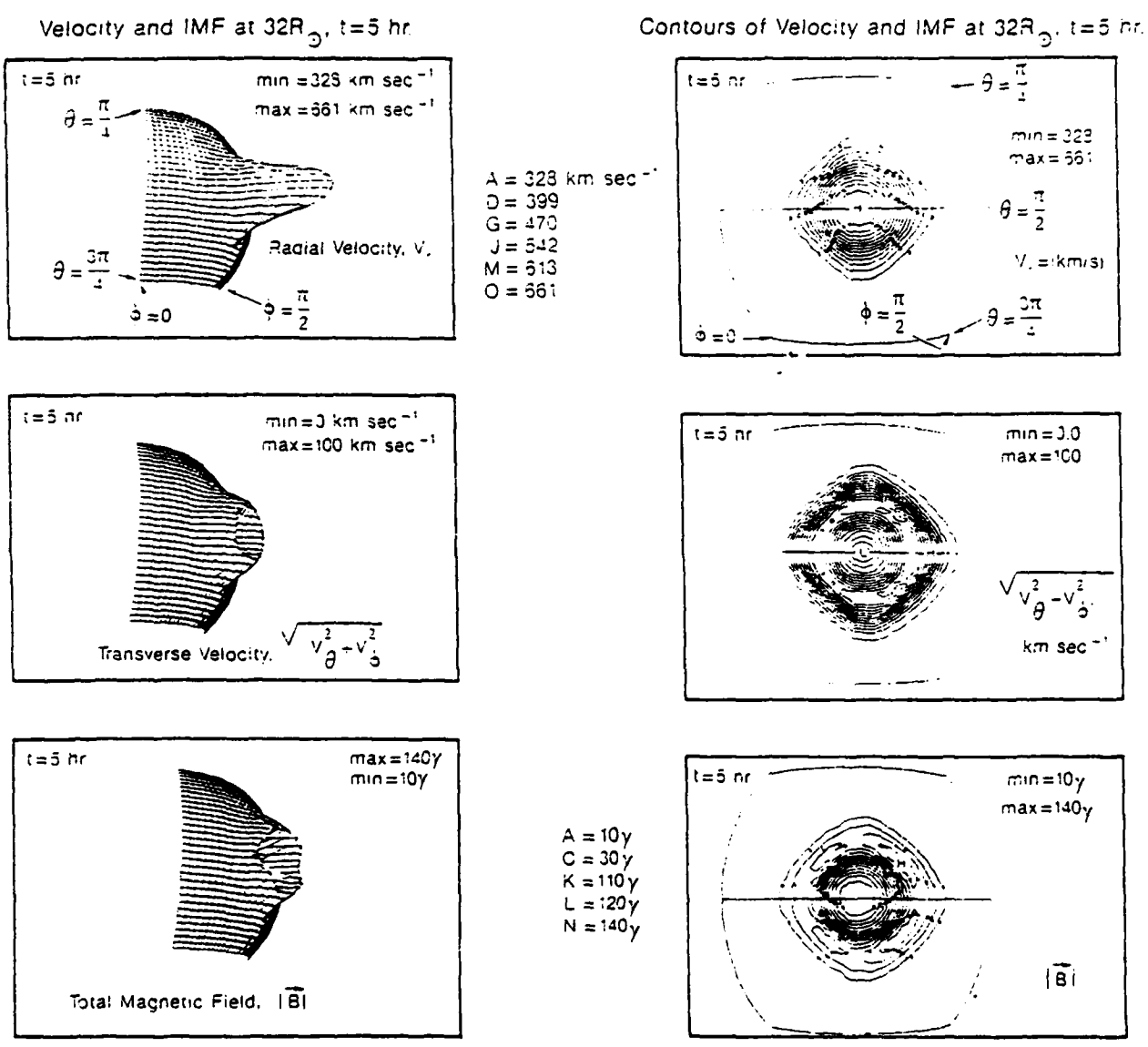

Figure 12.

Density Contours on $\phi - \theta$ Surfaces at Several Radial Locations and Times
$V_S = 1000$ km sec^{-1}

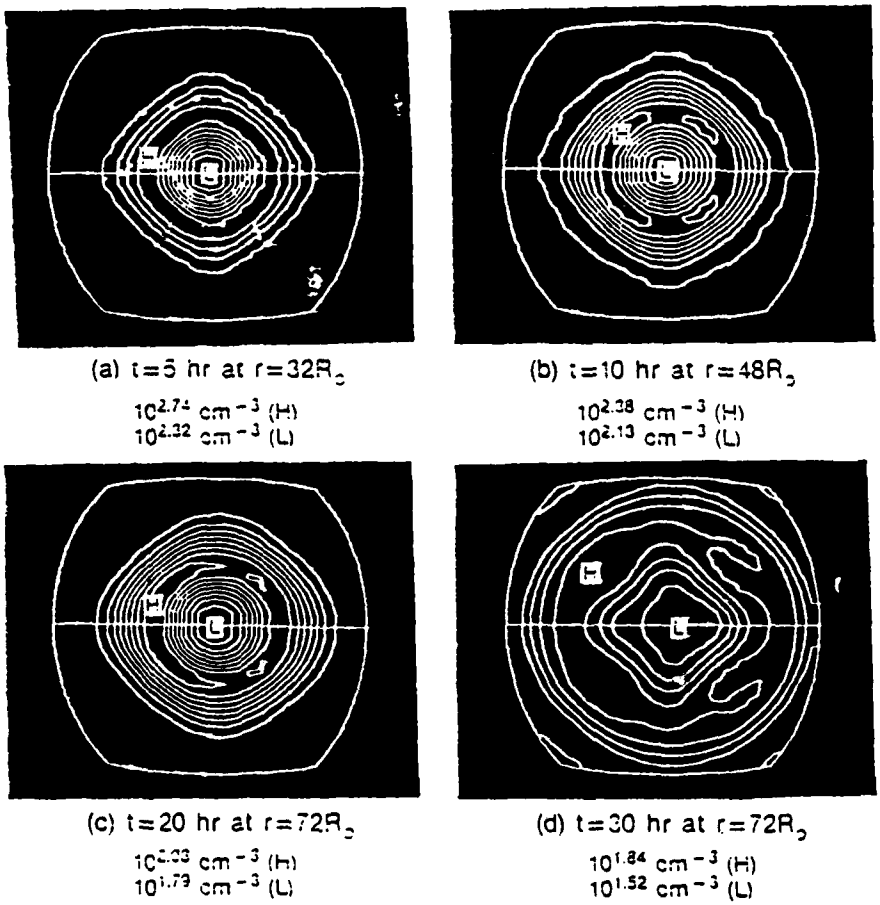

(a) t=5 hr at r=32$R_\odot$
$10^{2.74}$ cm^{-3} (H)
$10^{2.32}$ cm^{-3} (L)

(b) t=10 hr at r=48$R_\odot$
$10^{2.38}$ cm^{-3} (H)
$10^{2.13}$ cm^{-3} (L)

(c) t=20 hr at r=72$R_\odot$
$10^{2.03}$ cm^{-3} (H)
$10^{1.79}$ cm^{-3} (L)

(d) t=30 hr at r=72$R_\odot$
$10^{1.84}$ cm^{-3} (H)
$10^{1.52}$ cm^{-3} (L)

Figure 13.

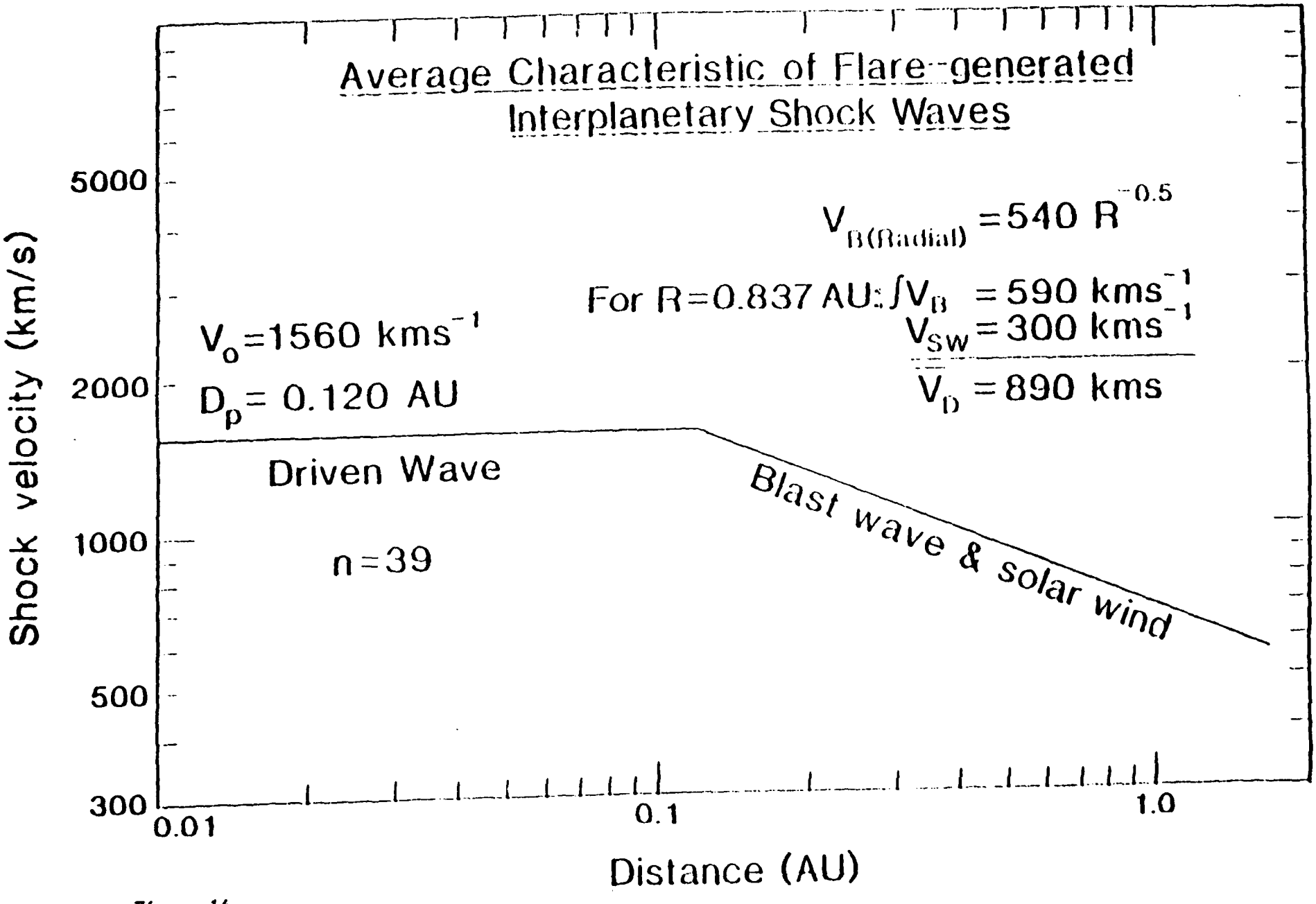
Average Characteristic of Flare-generated
Interplanetary Shock Waves
$V_{B(Radial)} = 540\ R^{-0.5}$
For R=0.837 AU: $\int V_B = 590$ kms^{-1}
$V_{SW} = 300$ kms^{-1}
$V_D = 890$ kms
$V_o = 1560$ kms^{-1}
$D_p = 0.120$ AU
Driven Wave
n=39
Blast wave & solar wind
Shock velocity (km/s)
5000
2000
1000
500
300
0.01
0.1
1.0
Distance (AU)

Figure 14.

STRATEGY FOR GEOMAGNETIC STORM PREDICTION — I

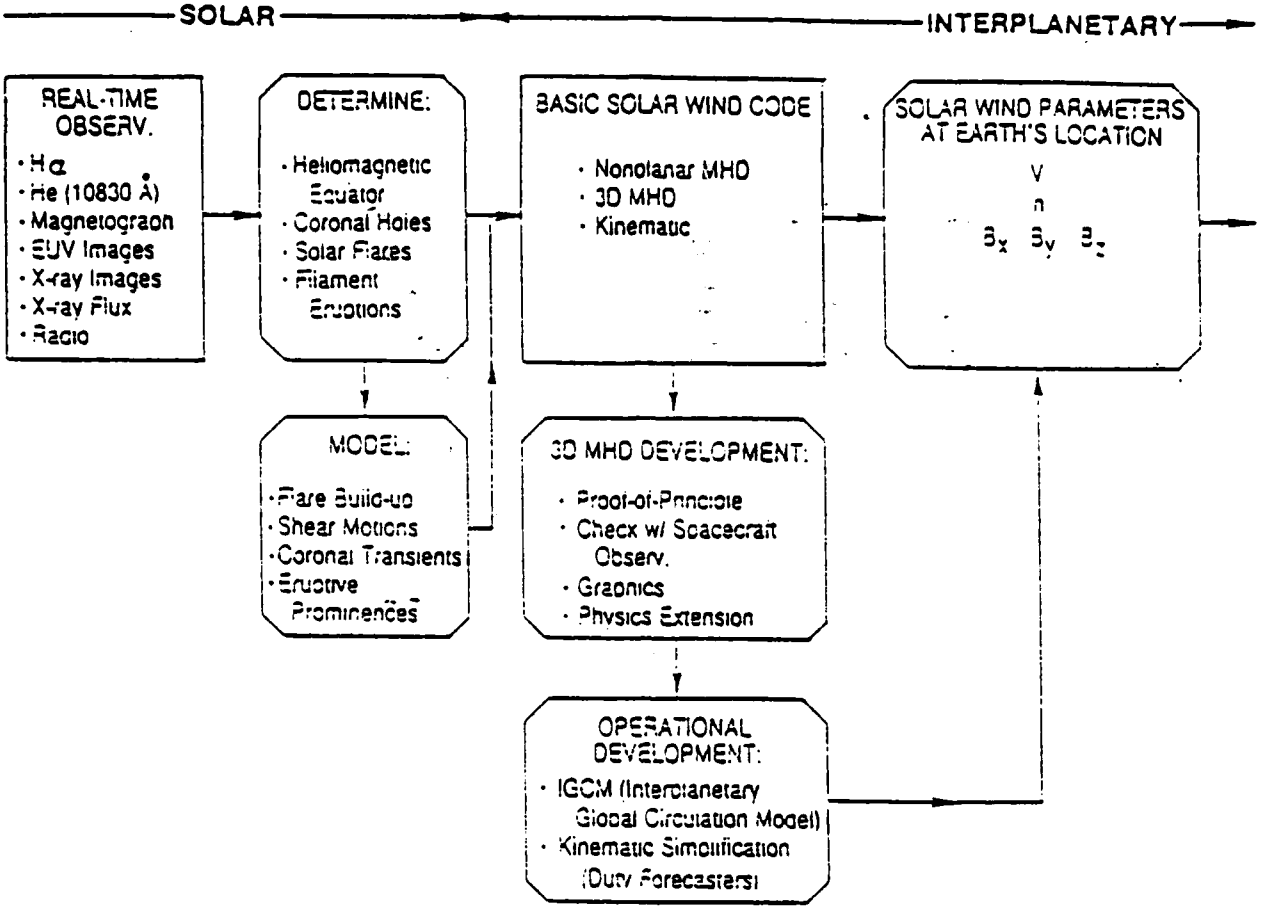

STRATEGY FOR GEOMAGNETIC STORM PREDICTION—II

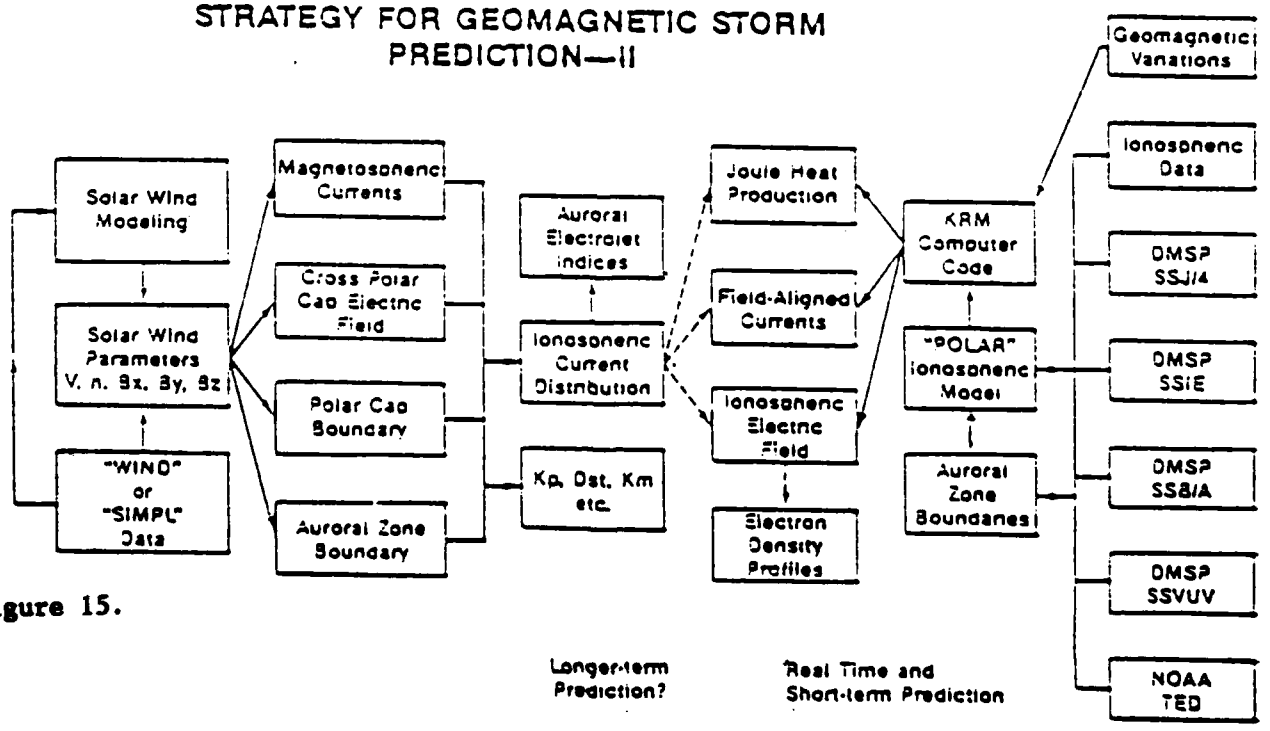

Figure 15.

END

10-86

DTIC